Indian Journal of Pure & Applied Physics
Vol. 64, October 2026, pp. 1154-1161
DOI: 10.56042/ijpap.v64i10.34303

Enhanced Performance of Piezoelectric Generator based on PVDF/ZnO/TiO_2 Composite Films for Energy Harvesting Applications

Hemendra Singh[a,b], Umang Berwal[a], Vinod Singh[a*], Ashok Kumar[a,c] & Richa Sharma[a]

[a]Department of Applied Physics, Delhi Technological University, Delhi 110 042, India

[b]Government Degree College Banjar, Kullu, Himachal Pradesh 175 123, India

[c]Department of Physics, Atma Ram Sanatan Dharma College, University of Delhi, New Delhi 110021, India

Received: 26th July 2026; accepted: 8th September 2026

The growing use of low-power electronic devices has highlighted the need for energy harvesting technologies that reduce dependence on conventional batteries. This work focuses on developing a piezoelectric energy generator incorporating poly vinylidene fluoride (PVDF) composite films with varying proportions (5 wt.%, 10 wt.% and 15 wt.%) of zinc oxide (ZnO) and fixed proportion (3 wt.%) of titanium dioxide (TiO_2) as dual fillers in various proportions. The composite films were characterized using techniques such as X-ray diffraction (XRD), Fourier Transform Infrared Spectroscopy (FTIR), Scanning Electron Microscopy (SEM), Atomic Force Microscopy (AFM) and Piezoelectric measurements. XRD analysis confirmed the presence of wurtzite ZnO and anatase TiO_2 along with the electroactive β-phase of PVDF. FTIR measurements further verified the enhancement in β-phase of PVDF on progressively increasing the filler loading. Further microstructural analysis of pristine PVDF and doped composite films were analyzed using SEM, and EDS analysis verified the incorporation of ZnO and TiO_2 in the PVDF. When subjected to identical mechanical force, ZTP10 fabricated device showed the maximum output among the Piezoelectric generators (PEGs).The open circuit voltage increased from 11V for undoped PVDF to 206 V for the ZTP10 device (10 wt.% ZnO & 3 wt.% TiO_2)- an 18.7-fold enhancement resulting from incorporation of dual fillers ZnO and TiO_2. The practical applicability of ZTP10 device was demonstrated using various human motions, it produced 28.4 V on fist thumping, 18.4 V on finger tapping, 3.4 V on wrist bending, and by glowing LEDs when tapped by hand, confirming its use in self-powered devices.

Keywords: Piezoelectric generators, X-ray diffraction (XRD), Scanning electron microscopy (SEM), Atomic force microscopy (AFM), Fourier transform infrared spectroscopy (FTIR)

1 Introduction

Among ambient energy harvesting techniques, nanogenerators that leverage triboelectric, piezoelectric, pyroelectric, and thermoelectric effects have been widely explored in recent years. In this context, piezoelectric generators have attracted significant attention for scavenging ambient energy as they do not require a temperature gradient or contact between materials unlike pyroelectric, thermoelectric and triboelectric generators. Piezoelectric devices offer superior durability, stable electric performance and can be used to make wearable devices and therefore are the most suitable candidates for mechanical energy harvesting[1–3].

The idea of piezoelectric generators was introduced by Z.L. Wang in 2006 through his seminal paper titled 'Piezoelectric Nanogenerators based on Zinc Oxide Nanowire Arrays' for converting mechanical vibrations to electrical energy[4]. Piezoelectric generators (PEGs) function on the principle of stress-induced polarization in materials, in which mechanical deformation leads to the separation of charges, resulting in the development of an electric potential. The choice of piezoelectric materials is critically important for the optimal functioning of PEGs, which are broadly divided into inorganic ceramics and organic polymers. Inorganic piezoelectric materials include Lead Zirconate Titanate (PZT)[5], Barium Titanate ($BaTiO_3$)[6], Potassium Sodium Niobate (KNN)[7], and Zinc Oxide (ZnO)[8]. Although inorganic ceramics exhibit higher electrical activity and high piezoelectric coefficients, their brittle nature severely limits their use in flexible, wearable electronics[9]. Flexible PEGs have been fabricated using organic piezoelectric materials based on organic polymers, especially PVDF[10], and its copolymers poly (vinylidene fluoride- tetrafluoroethylene) (P(VDF-TFE)[11], poly(vinylidene fluoride-trifluoroethylene) P(VDF-TrFE)[12], and Poly(vinylidene fluoride--

*Corresponding author: E-mail:vinodsingh@dtu.ac.in

hexafluoropropylene) (PVDF-HFP)[13]. These polymers are lightweight, mechanically flexible, chemically stable, biocompatible, and relatively easy to process[14].

PVDF is recognized for having five distinct crystalline forms, specifically the α, β, γ, δ, and " ε phases. Among these, the polar β-phase, characterized by an all-trans (TTTT) chain configuration where each -CF_2 dipole is oriented in the same direction, exhibits the most promising piezoelectric properties[15]. The solution casting process which is generally used for fabrication of flexible films, typically yields the non-polar α-phase, which only provides a moderate piezoelectric effect. Consequently, increasing the proportion of the β-phase is essential to enhance the electromechanical performance of PVDF-based PEGs[16].One of the most commonly used strategies to achieve crystallization in the β-phase of PVDF is through the incorporation of functional fillers or nanostructured additives in the PVDF matrix. Recent studies have demonstrated an enhancement in the polar phase by integrating fillers such as lead-based perovskites[17], lead-free ceramics[18], carbon-based additives[19], and metal oxides[20] into the PVDF matrix.

Among the metal oxide fillers explored, ZnO has attracted the most attention as it crystallizes in a non-centrosymmetric wurtzite crystal structure and has intrinsic piezoelectric properties[21].By incorporating ZnO into the PVDF matrix, the polar β-phase increases from 48.2% to 76.1% after filler loading[22]. An enhancement in β-phase to 87.2% on loading of 3 wt% ZnO into PVDF matrix was reported[23]. Another highly effective nanofiller in piezoelectric systems made of PVDF is TiO_2 as it is chemically and thermally stable and has a high dipole moment[24]. Adding titanium dioxide TiO_2 nanofillers to a PVDF matrix significantly enhances the electroactive β-phase content by 89% and improvement in piezoelectric performance of PVDF/TiO_2composite films[25].

Recent studies have shown that the incorporation of dual piezoelectric fillers in PVDF leads to better performance of generators as compared to single-filler systems. The enhancement of the piezoelectric properties arises from complementary mechanisms, wherein different fillers contribute through distinct pathways[26,27]. Therefore, in this study, we prepared PVDF films loaded with 0-15 wt.% ZnO and a fixed 3 wt.% TiO_2 by the solution casting process and characterised them using XRD, FTIR, SEM, EDS, and AFM and piezoelectric measurements. The output voltage of the PEGs was recorded for films of varying concentrations to determine whether the dual-filler approach could enhance the piezoelectric output and find the optimal filler loading for maximum output.

2 Experimental

2.1 Material

PVDF powder was used as the polymer matrix. ZnO (Fisher Scientific, 99% purity) and TiO_2 (Sigma Aldrich, 99.5% purity) were used as inorganic fillers. N,N-Dimethylformamide (DMF) solvent was used to dissolve the polymers.

2.2 Fabrication of ZnO/ TiO_2/PVDF Composite Flexible Films

The composite films were fabricated using solution casting process, as shown in Fig. 1 PVDF powder was first dissolved in DMF and magnetically stirred continuously for approximately 1.5 h until a clear, transparent solution was obtained[28]. In another beaker, ZnO and TiO_2 powders were dissolved in DMF and

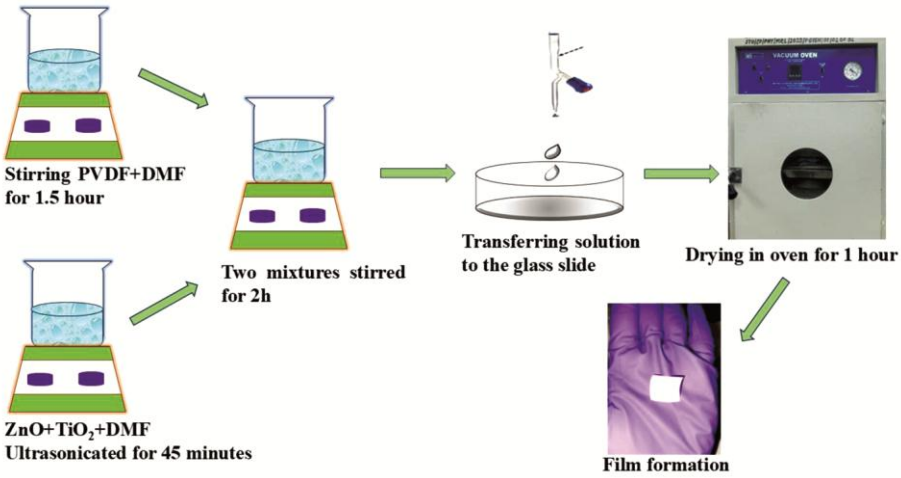


Fig. 1 — Synthesis of composites films with varying weight percentages of zno and tio_2 in pvdf using solution casting method

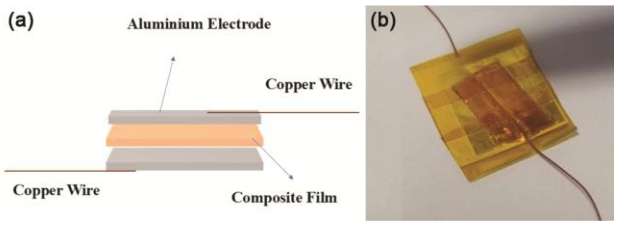


Fig. 2 — (a) Schematic illustration of Piezoelectric generator; and (b) The PEG device

ultrasonicated for 45 min to break up any particle clusters and achieve a well-dispersed suspension.

Subsequently, the dispersed suspension was mixed with the PVDF solution and subjected to magnetic for another two hours, until the fillers were evenly distributed throughout the polymer matrix[29]. Once the solution appeared homogeneous, it was gently transferred into a clean Petri dish for drying in an oven. After oven drying at 85 °C for approximately one hour, the solvent completely evaporated, resulting in the formation of flexible film. For ease of reference throughout this study, the films are labelled according to their filler content: ZTP0 for pure PVDF, and ZTP5 (5 wt% ZnO + 3 wt% TiO_2), ZTP10 (10 wt% ZnO + 3 wt% TiO_2) and ZTP15 (15 wt% ZnO + 3 wt% TiO_2).

2.3 Device Assembly

Once the composite film was ready, a piezoelectric generator was constructed by carefully placing conducting aluminium tape on both faces of the film to collect the generated charges. To complete the electrical setup, copper wires were attached to the terminals for measurements, as illustrated in Fig. 2. The entire setup was thenencased in Kapton tape to protect the device from moisture and everyday wear during handling[30].

2.4 Characterization

The crystalline phases present in the pure PVDF and PVDF/ZnO/TiO_2 composite films were investigated by XRD (Rigaku Ultima-IV) using Cu-Kα (λ=1.54 Å) radiation. FTIR (PerkinElmer FTIR spectrum II) was used for investigation of the β-phase content of composite films of various concentrations. Scanning electron microscopy examined film morphology. The elemental composition and distribution of zinc, titanium, and other constituent elements in the films were examined using energy-dispersive spectroscopy (EDS). AFM (Witec GmbH, Germany) was employed to evaluate theroughness of films.

The voltage generated by the PEGs was measured using a Tektronix MDO 500 digital oscilloscope.

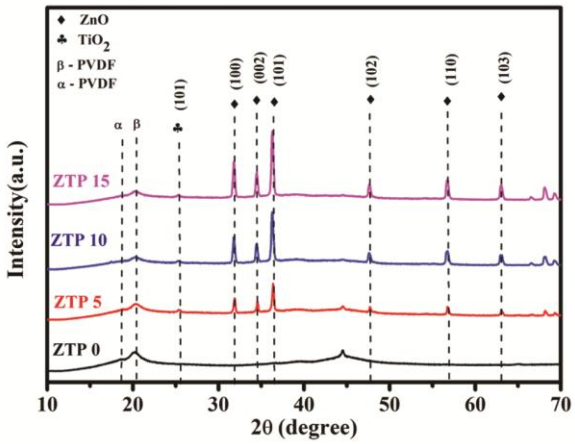


Fig. 3 — XRD patterns of varying concentration of ZnO/ TiO2/PVDF composite films

Voltages for different motions, such as finger tapping, fist thumping, finger bending, and hand tapping, were measured using digital storage oscilloscope, and for practical applications, piezoelectric generator was used to glow LEDs through hand tapping.

3 Results and Discussion

3.1 Structural Analysis of Composite Films

3.1.1 XRD Studies of Composite Films

The XRD patterns of all the films over the ranging from 10^o to 70^o along x-axis are shown in Fig. 3. The ZTP0 film shows a peak that corresponds to the α-phase at 18.4^o, in addition to a peak corresponding to β-phase at 20.3^o. In the composite films, the peaks observed at 31.6^o, 34.5^o, 36.2^o, 47.5^o, 56.6^o,and 63.0^o, that correspond to hexagonal wurtzite ZnO, which is in good agreement with JCPDS (card number 36-1451)[31–33]. The peak intensities increased on increasing the ZnO concentration from 5 to 15 wt%. Furthermore, a weaker peak was observed at 25.3^o that corresponded to the (101) plane of anatase TiO_2 (JCPDS 21-1272)[34]. The β-phase peak intensity increased considerably in the composites, whereas the α-phase weakened. Therefore, XRD analysis shows that incorporating dual fillers helps enhance the β-phase of PVDF.

3.1.2 SEM Studies of Composite Films

The SEM analysis revealed a smooth morphology for pure PVDF films Fig. 4(a) , SEM images Fig. 4(b-d) ZTP10 and ZTP15, respectively, show a homogeneous dispersion of dual fillers throughout the PVDF. As the concentration increased, ZTP15 exhibited filler agglomeration, indicating the optimal

loading of ZTP10 (10 wt% ZnO). A uniform distribution of fillers causes dipoles to align in a particular direction, which facilitates charge mobility and thus enhances the piezoelectric generator's performance[35–37].

Energy-dispersive X-ray Spectroscopy (EDS) was employed to map the elemental composition of the fabricated composite films. Pure PVDF, Fig. 5(a) shows only C and F as these are the only elements present in the polymer. The spectra of the composite films Fig. 5(b-d) display additional peaks corresponding to oxygen, titanium, and zinc, which arise from the incorporated TiO_2 and ZnO particles, confirming that fillers are incorporated into the polymer matrix and indicating an increased concentration of ZnO particles.

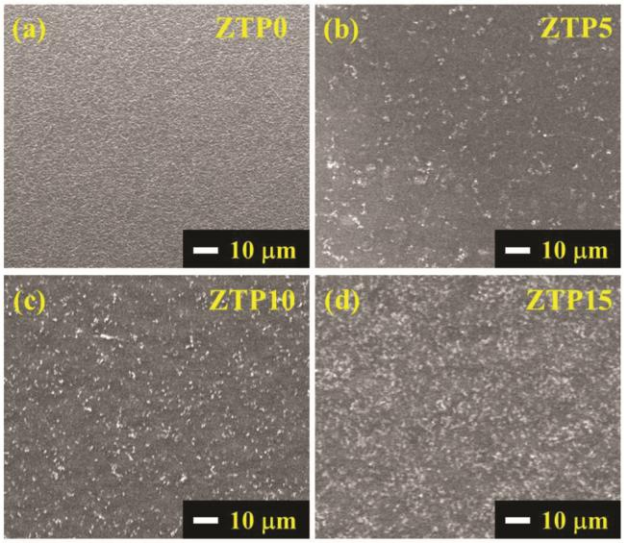


Fig. 5 — SEM images of (a) ZTP0 (b) ZTP5 (c) ZTP10; and (d) ZTP15 composite films

3.1.3 AFM Analysis of Composite Films

The analysis of AFM images of films as shown in Fig. 6 using WiTec Project four software gives the surface roughness of ZTP0 as 270 nm and ZTP10 as 730 nm. This increase in surface roughness leads to an increased surface charge density, resulting in enhanced piezoelectric performance[38,39].

3.1.4 FTIR Analysis of Composite Films

FTIR absorbance spectra of all the films in the wavenumber range 600-1500 cm^{-1} along x-axis is shown in Fig. 7. The peaks for the α-phase of PVDF were observed at 764 cm^{-1} and 1401 cm^{-1}, and the corresponding β-phase peaks were observed at 835 cm^{-1}, 873 cm^{-1},1070 cm^{-1}, 1166 cm^{-1}, and 1231 cm^{-1}. For the calculation of the relative β-phase content of the films using the Beer-Lambert law, peaks corresponding to the α- and β-phases at 764 cm^{-1}, and 835 cm^{-1}, respectively were used[15,40–42].

$$F(\beta) = \frac{A_\beta}{(\frac{K_\beta}{K_\alpha})A_\alpha + A_\beta} \quad \text{... (1)}$$

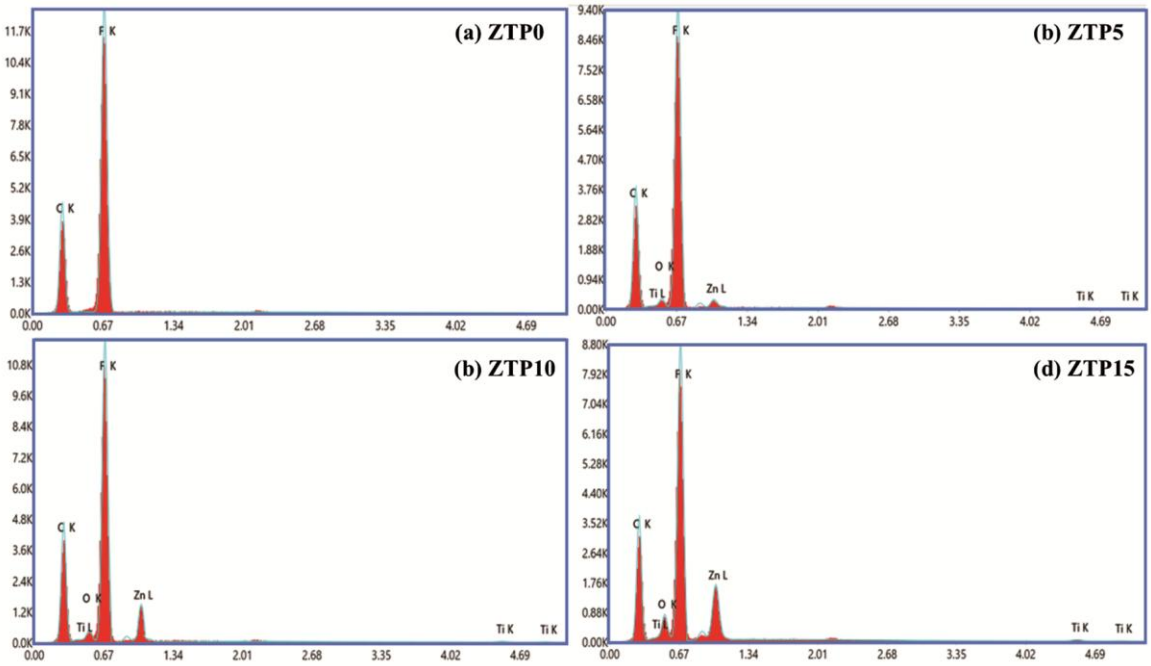


Fig. 4 — EDS images of (a) ZTP0 (b) ZTP5 (c) ZTP10; and (d) ZTP15 composite films

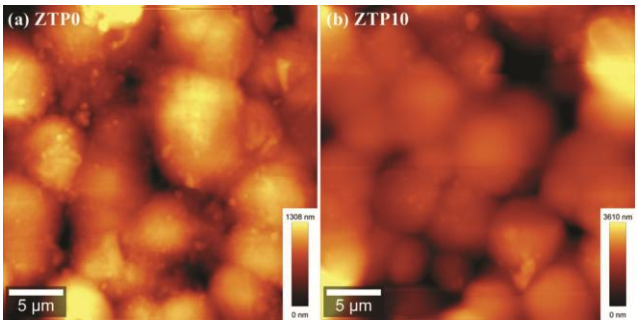


Fig.6 — AFM micrographs of (a) ZTP0; and (b) ZTP10 films

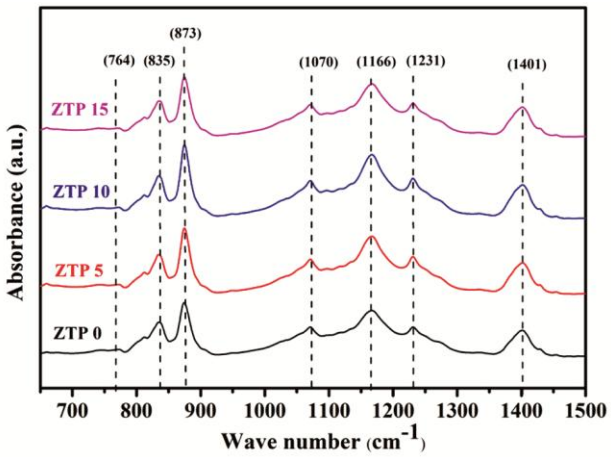


Fig. 7 — FTIR spectra of ZnO/ TiO_2/PVDF composite films

where, A_α and A_β denote absorbance values at 765 cm^{-1} and 835 cm^{-1} respectively. The absorbance coefficient values are $K_\alpha = 7.7 \times 10^4 cm^2/mol$ and $K_\beta = 6.1 \times 10^4 cm^2/mol$.

In this study, the calculated β-phase values were 42%, 64%, 80%, and 72% for ZTP0, ZTP5, ZTP10, and ZTP15, respectively. The decrease in the β-phase content from the maximum (80%) for ZTP10 to 72% for ZTP15 can be attributed to the formation of agglomerates at higher filler loadings, as confirmed by the SEM analysis[43].

3.2 Voltage Output of the Piezoelectric Generator

The open-circuit voltage of the fabricated piezoelectric generator was measured during periodic hand tapping using a digital storage oscilloscope (MDO 500, Tektronix). The time-dependent voltage waveforms were depicted in Fig. 8. The output voltage increased on incorporation of dual fillers, reaching a peak of 206 V for ZTP10. The voltage trend observed across the series closely follows the measured β-phase content of the films. The decrease in the ZTP15 output voltage can be attributed to a reduction in β the phase content owing to the formation of agglomerates at higher concentrations, as confirmed by SEM[36].

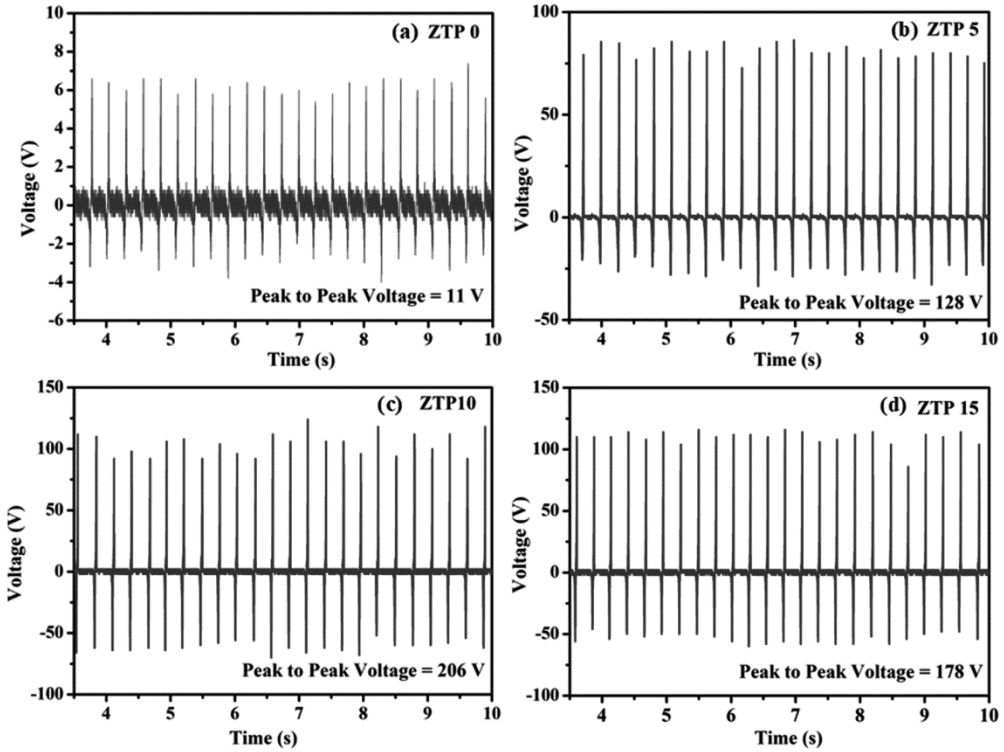


Fig. 8 — Open Circuit Voltage of Piezoelectric generator using different composite films (a) ZTP0, (b) ZTP5, (c) ZTP10; and (d) ZTP15

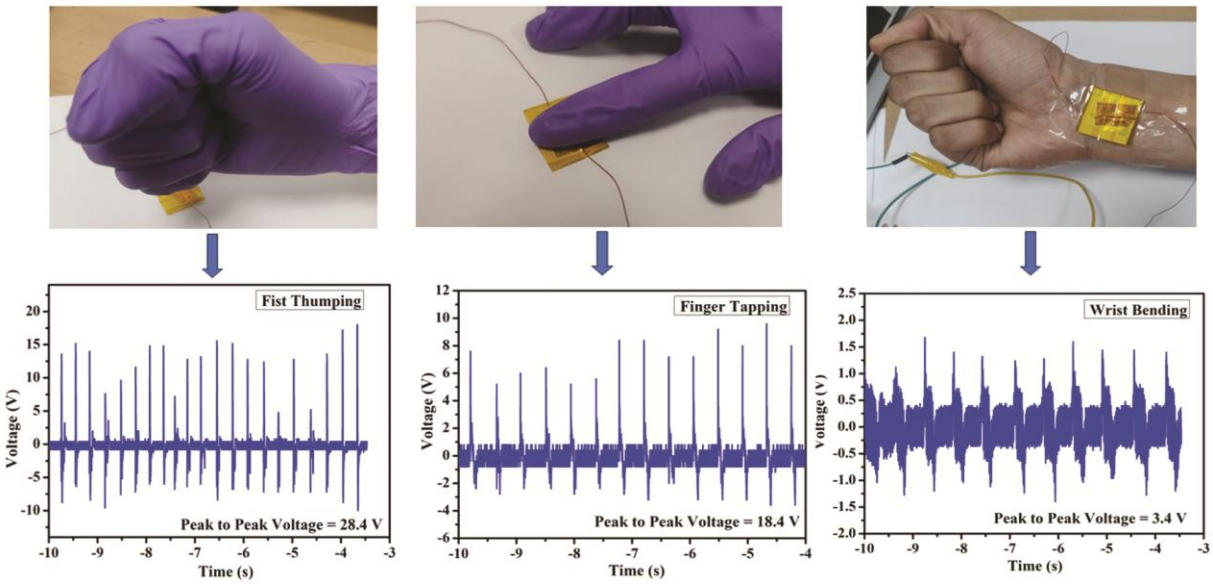


Fig. 9 — Output Voltage of ZTP10 device in response to (a) Fist Thumping (b) Finger Tapping; and (c) Wrist Bending

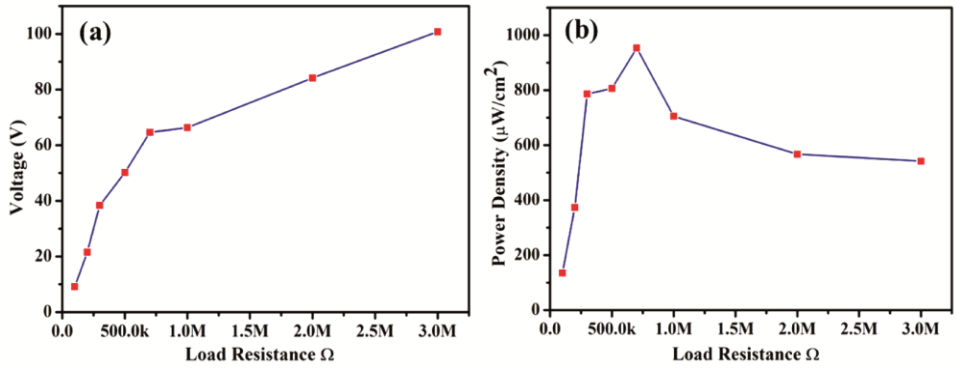


Fig. 10 — Variation of (a) Output Voltage; and (b) Power density with load resistance

To study the versatility of the device, the best-performing device (ZTP10) was subjected to fist-thumping, finger-tapping, and wrist-bending, the device's electrical output was measured for each stimulus, and the resulting voltages are shown in Fig. 9. Fist thumping and finger tapping involve lesser force than hand tapping; therefore, the output voltages were relatively lowery at 28.4 V and 18.4 V, respectively. Wrist bending, characterized by a slow, distributed load, yielded only 3.4 V, because the resulting strain on the piezoelectric crystal is minimal. These results show that the output of the PEG depends on the magnitude of the applied mechanical force; therefore, these devices can be used in sensor applications[44,45].

3.3 Power Measurement of PEG Device

The electrical power output of the ZTP10 PEG was studied by varying the load resistance to identify the optimum operating condition for maximum power transfer Figure 10 shows how the output voltage and power density change with load resistance. Thepeak-to-peak voltage across the load resistance was measured to be 9.2 V at 100 kΩ and increased to 100.8 V at 3 MΩ. The power density was calculated using formula[46];

$$P = \frac{V^2}{RA} \quad \ldots (2)$$

Here, Area of the device $A = 6.25$ cm^2. The power density initially increased on increasing load resistance, reaching a peak value of 953.58 μW/cm^2 at 700 kΩ, and then decreased with further increasing load resistance. This behaviour is consistent with maximum power transfer theorem, according to which the maximum power density is obtained at the optimal load resistance, where the external load resistance matches PEG's internal impedance of the PEG[47–49].

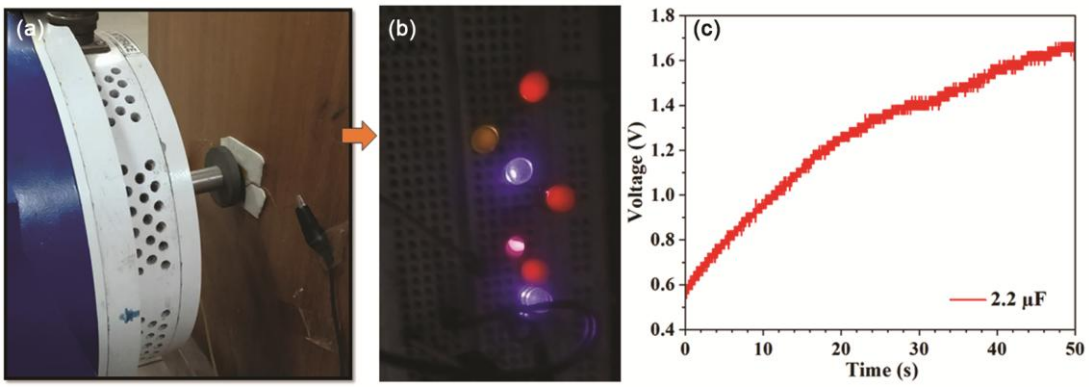


Fig. 11 — (a) Mechanical force applied by shaker on ZTP 10 device (b) Glowing of LEDs; and (c) Charging of capacitor by PEG device

3.4 Practical Application of PEG Device with ZTP10 Composite Film

The fabricated PEG device demonstrated the practical energy harvesting capability by responding to different mechanical motions such as Fist thumping, finger tapping and wrist bending. In addition to this seven LEDs of different colours (namely red yellow and blue) were illustrated Fig. 11 (b) further Fig. 11 (c) demonstrates charging of a capacitor of 2.2 µF.

4 Conclusion

Fabricated flexible piezoelectric generators (PEGs) from composite films of PVDF/ZnO/TiO_2 using solution-casting process. The films were examined using XRD, SEM, EDS, AFM, FTIR and piezoelectric measurements. Incorporation of ZnO and TiO_2increased the β-phaseof PVDF, as confirmed by XRD and FTIR analysis. The higher β-phase fraction improved the performance of PEGs. The PEG device containing 10 wt.% ZnO and 3 wt.% TiO_2 delivered maximum output of 206 V and power density of 953.58 µW/cm^2 across an optimal external resistance of 700 kΩ and shown practical applicability by charging a capacitor of 2.2 µF and glowing 7 LEDs. These results shows that use of dual fillers ZnO and TiO_2 in PVDF matrix creates a synergistic effect, thereby improving the capabilities of the PEGs. Owing to their enhanced piezoelectric response, the developed PEGs are well suited for wearable electronics and ambient energy harvesting.

References

1 Mohith S, Upadhya A R, Navin K P, Kulkarni S M & Rao M, *Smart Mater Struct*, 30 (2020) 13002.
2 Sezer N & Koç M, *Nano Energy*, 80 (2021) 105567.
3 Anton S R & Sodano H A, *Smart Mater Struct*, 16 (2007) R1.
4 Wang Z L & Song J, *Sci*, 312 (2006) 242.
5 Kang M-G, Jung W-S, Kang C-Y & Yoon S-J, *Actuators*, 5 (2016) 1.
6 Nunes-Pereira J, *et al.*, *Compos B Eng*, 72 (2015) 130.
7 Wu J, Xiao D & Zhu J, *Chem Rev*,115 (2015) 2559.
8 Mahapatra A, Ajimsha R S, Deepak D & Misra P, *Sci Rep*, 14 (2024) 11871.
9 Ramadan K S, Sameoto D & Evoy S, *Smart Mater Struct*, 23 (2014) 33001.
10 Song J, Zhao G, Li B & Wang J, *Heliyon* 3 (2017) 1.
11 Fan X, *et al.*, *React Funct Polym*,180 (2022) 105391.
12 Zhang Q M, Bharti V & Zhao X, *Sci*, 280(1998) 2101.
13 Parangusan H, Ponnamma D & Al-Maadeed M A A, *Sci Rep*, 8 (2018) 754.
14 Sukumaran S *et al.*, *J Intell Mater Syst Struct*, 32 (2021) 746.
15 Martins P, Lopes A C & Lanceros-Mendez S, *Prog Polym Sci*, 39 (2014) 683.
16 Cerrada M L, Arranz-Andrés J, Caballero-González A, Blázquez-Blázquez E & Pérez E, *Polymers (Basel)*, 15 (2023) 1.
17 Paralı L, Koç M & Akça E, *Ceram Int*, 49 (2023) 18388.
18 Patra A, Pal A & Sen S, *Ceram Int*, 44 (2018) 11196.
19 Zhu M, Liu Q, Wong W-Y & Xu L, *Adv Mater*, 37 (2025) 2419970.
20 Sebastian T & Clemens F, *Metal Oxide-Based Nanofibers and Their Appl*, (2022) 215–246 doi:10.1016/B978-0-12-820629-4.00002-3.
21 Duraccio D & Malucelli G, *Discov Mater*, 6 (2026) 44.
22 Singh H H, Singh S & Khare N, *Polym Adv Technol*, 29 (2018) 143.
23 Hari M A, Karumuthil S C, Varghese S & Rajan L, *IEEE Sens J*, 22 (2022) 9336.
24 Alam M M, Sultana A & Mandal D, *ACS Appl Energy Mater*, 1 (2018) 3103.
25 Kulkarni N D & Kumari P, *Mater Res Bull*, 157 (2023) 112039.
26 Naik RS M & Chavan S, *Eng Res Express*, 3 (2021) 025003.
27 Sabry R S & Hussein A D, *Polym Test*,79 (2019) 106001.
28 Verma K & Sharma R, *Chin J Phys*, 84 (2023) 198.
29 Kumar A & Sharma R, *Curr Appl Phys*, 68 (2024) 159.
30 Kumar A & Sharma R, *Mater Sci Semicond Process*, 199 (2025) 109814.

31 Krishna Reddy G, Jagannatha Reddy A, Hari Krishna R, Nagabhushana B M & Gopal G R, *J Asian Ceramic Soc*, 5 (2017) 350.
32 Fang L *et al.*, *Superlattic Microstruct*, 75 (2014) 324.
33 Etape E P*et al.*, *J Nanomater*,2018 (2018) 9072325.
34 Xu H, Li G, Zhu G, Zhu K & Jin S, *Catal Commun*, 62 (2015) 52.
35 Verma K & Sharma R, *Bullet Mater Sci*, 47 (2024) 38.
36 Biswas P, *et al.*, *ACS Sustain Chem Eng*, 7 (2019) 4801.
37 Berwal U, Singh V & Sharma R, *J Lumin*, 257 (2023) 119687.
38 Gogneau N, *et al.*, *phys status solid Rapid Res Lett*, 8 (2014) 414.
39 Singh H H & Khare N, *Nano Energy*, 51 (2018) 216.
40 Bhatt A, *et al.*, *J Alloys Compd*, 960 (2023) 170664.
41 Guo D, *et al.*, *J Materiomics*, 6 (2020) 563.
42 Prabhakaran T & Hemalatha J, *Mater Chem Phys*, 137 (2013) 781.
43 Nardekar S S, Krishnamoorthy K, Pazhamalai P, Sahoo S & Jae Kim S, *Nano Energy* 93 (2022) 106869.
44 Mitrovic M, Carman GP & Straub K F, *Int J Solids Struct*, 38 (2001) 4357.
45 Halim M A & Park J Y, *Sens Actuators A Phys*, 208 (2014) 56.
46 Sadaf M U K, *et al.*, *Nano Trends*,8 (2024)100063.
47 Rafique S, *et al.*, *Curr Appl Phys*, 21 (2021) 72.
48 Cao S, Zou H, Jiang B, Li M & Yuan Q, *Nano Energy*, 102 (2022) 107635.
49 Faraz M, Singh H H & Khare N *J Alloys Compd*, 890 (2022) 161840.